MONODORA MYRISTICA EXTRACT: A SUSTAINABLE SUBSTITUTE TO ZINC PHOSPHATE FOR EPOXY COATINGS.

Macdenis Onyekachi Egbuhuzor[1,2,*], Christogonus Oudney Akalezi[2,3], Chinyere Ada Madu[3,4] Emmanuel Emeka Oguzie[2,3]

[*1]Department of Metallurgical and Materials Engineering, the University of Nigeria, Nsukka, Enugu State, 410001, Nigeria
[2]Africa Centre of Excellence for Future Energies and Electrochemical Systems (ACEFUELS), Federal University of Technology Owerri, Imo State, Nigeria
[3]Department of Chemistry, Federal University of Technology Owerri, Imo State, Nigeria
[4]Department of Physics, Federal University of Technology Owerri, Imo State, Nigeria

[*] Corresponding Author: [Onyekachi.egbuhuzor@unn.edu.ng]
https://orcid.org/0000-0002-5103-314X

ABSTRACT
This research explored the use of monodora myristica (African nutmeg) extract as a sustainable and biodegradable substitute for zinc phosphate in epoxy coatings. A market standard coating formulation was used, and the percentage of zinc phosphate in the coating was substituted with Monodora myristica extract (MME). The coatings were applied to the mild steel substrate and allowed to dry in the open air. Fourier Transform Infrared Spectroscopy (FTIR) confirmed the presence of functional groups and bioactive ingredients that assist in both coatings' anti-corrosion properties. Morphological properties were studied using Atomic Force Microscopy (AFM), Scanning Electron Microscopy (SEM). Thermal studies were carried out using a Differential Scanning Calorimeter (DSC), while the electrochemical test utilised the rapid electrochemical assessment of paints (REAP) test. Finally, Computational studies were performed using density functional theory (DFT) and molecular Dynamics simulations (MDS). The results of the AFM showed a surface roughness of 1.15nm and 0.97nm for epoxy coated with zinc phosphate and extract, respectively. The extract-based coating had a slightly higher hardness value (100.3 HRB) compared to the market standard, with a micro hardness of 99.2 HRB. The DSC results showed that both coatings exhibit minor low-temperature features (~50–80 °C). The zinc phosphate formulation maintains a gradual heat-flow profile, while *Monodora* extract coating shows an earlier and steadier increase in heat flow. The (REAP tests showed a very close coating solution resistance of 7.43 ohms and 8.99 ohms, and a very close Relative Time To Failure, TTF (hrs) of 1240.4. and 1090.23 hrs. for both the epoxy/zinc phosphate and epoxy/extract coatings, respectively. The study demonstrates that coatings formulated with MME exhibit comparable morphological, thermal, and electrochemical properties to zinc phosphate-based coatings, indicating that MME can effectively replace hazardous substances without compromising performance.

Keywords: Monodora Myristica; Extract; Coatings; Zinc Phosphate; Eco-friendly; Epoxy resin

Received: March 15, 2025. Revised: June 21, 2025. Accepted: August 17, 2025. Published: October 01,2025.

1.0 INTRODUCTION

Metals corrode when they come in contact with the environment, forcing them to revert to their stable inorganic states like oxides, sulphides, carbonates, etc.(Hansson 2011). As metals find applications in every facet of life, they face degradation attacks from these environments. Corrosion constitutes a safety risk to our critical infrastructure, causing economic losses due to repairs, maintenance, replacement, and labour (Bastidas, 2020). Corrosion causes functional impairment, structural failures, a reduced lifespan of materials, increased maintenance costs, and sometimes loss of life.

To reduce the corrosion of metals, we must control the interaction of the metal with the environment by modifying the interface between the environment and the metal. This can be done through material design, protective coating, cathodic protection, and corrosion inhibitors (Bansal et al., 2016).

Inhibitors have been widely used to control corrosion. They are substances added in small amounts to reduce the menace of corrosion by reducing anodic, cathodic or both reaction rates, thereby forming protective films on metal surfaces(Nguyen et al., 2024). They are classified as either inorganic or organic corrosion inhibitors. Inorganic inhibitors form protective films on the surface of the metal substrates and so prevent the formation of corrosion cells. Examples include metal salts of phosphates, tungstates, nitrates, silicates, molybdates, bromates, and chromates(Al-Amiery, Isahak, and Al-Azzawi 2023). Organic inhibitors, on the other hand, are absorbed on the metal surface to form a barrier coating, preventing a corrosive environment's direct attack on the metal. They contain amines, alcohols, and amino acids. Organic inhibitors contain functional groups that interact with the metal substrate, forming protective layers on the substrate, thereby protecting it from corrosion(R. Holla et al., 2024; Al-Amiery et al., 2023).

Plant extracts and oils are good examples of organic corrosion inhibitors. They have polar functional groups containing heteroatoms such as O, S, F, N, P (Singh, Ebenso, and Quraishi 2012) present in phytochemical compounds such as tannin, flavonoids, terpenoids, naringenin, steroids, rutin, phloroglucinol, resveratrol, anthocyanin, etc., with good corrosion inhibition effects, forming defensive films on the metal.

Surface coatings have been applied to protect metal surfaces by acting as a barrier against corrosive exposure. They include drying oils, paints, synthetic clear coats, varnishes and others and are applied to the surface of materials to protect them from harsh environmental conditions. Coatings contain binder, solvents, additives, pigments, catalysts, diluents, antioxidants, etc., added in the right proportions to get a perfect mix with better coating properties(Sørensen et al., 2009). They are always in powder, paste, colloidal or liquid form that, when applied to a substrate, forms a film possessing decorative, protective, and other specific properties (Humar, 2017).

Zinc phosphate has long been used as a major additive and corrosion inhibitor in protective coatings. It has the property of reducing paint-to-metal reactions by forming a barrier between the substrate and the paint, and it enhances paint adhesion by providing a secure bond for the paint. However, its environmental impact and toxicity raise concerns. Zinc phosphate can leach out over time, reducing the long-term effectiveness, inhibiting corrosion only through barrier and passivation and not by sacrificial protection(Leite et al., 2005). This work explores the phytochemical composition and bioactive compounds in monodora myristica extract (MME) and its corrosion inhibition potential in coatings. Also, the properties and performance results of the coatings with the extracts are compared with those containing zinc phosphates in terms of their morphology, electrochemistry and hardness properties. Computational studies were used to ascertain the molecular interaction between the coating compositions and the steel substrate.

2.0 MATERIALS AND METHODS

2.1 Materials

Materials used include monodora myristica extract gotten from the dried seeds of monodora myristica or African Nutmeg and purchased from the Ogige market, Nsukka, Enugu State, Nigeria, distilled water, analytical grades of petroleum ether, N-hexane, N-butanol, epoxy resin, genapol 700, polyethylene glycol (PEG), titanium oxide, zinc phosphate, barite, natrosol, versamid 125, solvent naphtha, talk, mild steel coupons, etc. Also, the equipment used includes a Soxhlet extractor, beakers, volumetric flasks, a desiccator, a funnel, a digital weighing balance, an FTIR spectrophotometer, GC-MS analysers, a digestion flask, a rotatory vacuum evaporator (Thermotech, Buchi type model th-012), a grinding machine, glass wool, a hotplate, transmission electron microscope, scanning electron microscope, electrochemical workstation, atomic force microscope, electric mixer, and UV-Vis spectrophotometer.

2.2 Methods

2.2.1 Preparation of the extract

The seeds of the monodora myristica were sourced from Nsukka town, Enugu state, Nigeria. They were collected in bulk, washed, and shade-dried. The dried samples were ground into powder. 1000g of the powder was macerated in 1500ml of petroleum ether solvent, and the mixture was extracted using a Soxhlet extractor. The sample mixture was extracted for 72 hours. The extract was filtered and then dried at low room temperature under pressure in a rotary vacuum evaporator (Thermotech, buchi type model th-012). The extracts were concentrated and then subjected to column chromatography, and the product of column chromatography was subjected to phytochemical screening using GC-FID and GC-MS. The extract was stored correctly in the desiccator for further experimental use and analysis.

2.2.2 Paint formulation

The paint composition is made up of two parts. The first part contains the epoxy resin and other additives, while the second part is the curing agent. Normal market standards were purchased and used as a base formulation for the coating. The first part comprises epoxy resin, genapol 700, zinc phosphate, barites, talc, natrosol, N-butanol, solvent naphtha, deformer, formalin, and titanium oxide. These are put in the right proportion by weight percentage in a beaker and stirred thoroughly using an electric mixer until a homogeneous mix is obtained. Also, the extract is used to substitute for the zinc phosphate in the coating formulation and stirred well until a complete blend or homogenised coating is formed. The second part, which is the curing agent, is made up of Versamid 125, N-butanol, and solvent naphtha, mixed also in the right proportion by volume. The first part, comprising the resin and the additives, is combined with the second part (curing agent) to form a complete coat. The coating is used on a well-prepared steel substrate and is characterized. Also, another coating is formed in the same proportion as above, but rather, the zinc phosphate in the market standard was substituted with the extract, mixed as above. The prepared coating is also cured using the second part of the coating and then applied to a metal substrate.

2.2.3 Metal preparation and spraying

The elemental analysis of the steel was conducted at the Defence Industries Corporation of Nigeria (DICON), Kaduna, Kaduna State, Nigeria, which gave us information about the elemental composition of the steel. The steel was then press-cut into coupons, degreased by washing in ethanol and polished with emery paper. The metal coupons were then rewashed in ethanol, rinsed in acetone to dry, and then stored in a desiccator before spraying with the formulated and cured coatings (Egbuhuzor et al., 2020).

2.2.4 Rapid electrochemical assessment of paints (REAP)

The REAP test was conducted on a scribed and unscribed coated steel substrate; the coating capacitance at zero and at 24 hours using an impedance measurement was recorded. Also, a 24-hour disbanding test to determine the corrosion resistance (Rcorr), the coating capacitance at zero hour (C_{c0}), the coating capacitance at 24 hours (C_{c24}), coating water uptake (%V), the disbanding rate (dx/dt) and the coating's relative time to fail (TTF) was carried out. The coating water uptake, disbanding rate, and relative time to fail of the coated substrate were then calculated using equations 1, 2, and 3, respectively(Buchheit et al., 1998).

1.0 Coating water update (%V) $=100\left[\frac{\log\{(Cc0)/logC24\}}{log80}\right]$ 1

2.0 Disbonding rate (x/dt) $= \frac{average\ with\ of\ scribed\ mark\ (mm)}{\frac{total\ time\ (hrs)}{2}}$ 2

3.0 Relative Time To Failure (RTTF) = - 830.1 + 118 log (R) - 169.2 log (dx / dt) - 48.03 ∗ %V 3

2.2.5 Surface Studies

Surface morphologies of the coated metal substrates with coatings containing zinc phosphate resin plus other additives and those containing the extract plus other additives were studied to examine the surface appearance and interactions of the coatings on the metal surface. Atomic force microscopy (Stromilingo DIY AFM) was used for the surface roughness, and the AFM was analysed with Gwydion software to obtain the 3-D images of the coated surfaces. Transmission electron microscopy (TEM) was conducted to study the crystal size of the coating materials, while scanning electron microscopy/energy dispersive spectroscopy (SEM-EDS) was used for surface morphology and elemental composition of the coatings.

2.2.6 Computational Studies

Computational studies using density functional theory and molecular dynamics simulations are used to probe how the different coating formulations (resin/additives/inhibitors/nanoparticles) interact with a mild steel surface and to compute the adsorption energies, preferred binding sites of the coating molecules, quantify charge transfer interfacial bonding nature, study the structural arrangement, dynamics and barrier properties of a thin coating layer on iron and at the same time provide observables that can be compared to experimental adsorption energies binding geometries, predicted spectroscopic signatures, water permeability and ion diffusion coefficients**.**

Materials Studio 4.0 was used for the quantum chemistry analysis, which included Atomistic Forcite Quench (AFQ) and DMol3. The phytochemical components of Monodora myristica extract, including methyl ester, hexadecanoic acid, methyl tetradecane, 9-octadecenoic acid, zinc phosphate, silver and copper nanoparticles, and a steel (Fe110) crystal, were subjected to geometry optimisation. A delocalized internal coordinate optimiser was used in this optimisation. Using Forcite Quench and the COMPASS forcefield, molecular dynamics simulations were run to simulate the interfacial interactions between the coating molecules and a Fe(110) crystal. The stimulation parameters were set up as described earlier. Interaction energy (EBind), global hardness and softness, electrophilicity, and the quantity of electrons transported, including other quantum parameters, were all calculated as part of the investigation.

2.2.7 Mechanical Test

The dried, coated steel substrate was cleaned to keep it free from dirt. The machine was set to the appropriate scale and parameters according to the thickness of the coat. The indenter was a steel ball of 100kgF weight. The metal substrate was placed firmly on the anvil of the tester. The indenter was lowered until it made contact with the coated steel substrate. The minor load was applied first to establish a zero reference point, and then the significant load was applied and held for a dwell time as specified for the Rockwell scale. Then the displayed hardness value was recorded. The test was repeated at different spot locations on the coated steel surface, and the average value was recorded. The tests followed the American Standard of Testing and Measurement ASTM E18.

3.0RESULTS AND DISCUSSIONS

3.1 Extraction and Photochemical Analysis.

The FTIR spectrum of the *Monodora myristica* seed extract in Figure 1 was analysed to identify the key functional groups present and infer its phytochemical composition. The spectrum revealed several characteristic absorption bands indicative of a complex mixture of bioactive constituents. A broad absorption band associated with antioxidant capacity observed at approximately 3420 cm^{-1} is attributed to O–H and N–H stretching vibrations, indicating the presence of hydroxyl groups of alcohols, phenolic compounds and amine groups from alkaloids and proteins. The strong absorptions in the region 2920–2850 cm^{-1} are characteristic of aliphatic C–H stretching vibrations (–CH_2– and –CH_3 groups), which are typical of long-chain fatty acids and lipids, consistent with the seed's known oil-rich nature. There is a sharp peak at 1740 cm^{-1} assigned to the C=O stretching vibration of esters, which confirms the lipid content in the extract. The absorption at 1635–1650 cm^{-1} can be ascribed to C=C stretching vibrations of alkenes in terpenoids or aromatic rings in flavonoids(Sahu & Haris, 2017). This region also confirms the presence of amide as assigned in the C=O stretching of proteins. Peaks in the range 1450–1375 cm^{-1} correspond to C–H bending vibrations of aliphatic hydrocarbon chains. Also, multiple bands in the 1240–1020 cm^{-1} region are due to C–O stretching vibrations of

alcohols, esters, and ethers, indicating the presence of polysaccharides, glycosides, and other oxygenated compounds. Finally, the fingerprint region (< 800 cm^{-1}) showed aromatic C–H bending vibrations, confirming the presence of aromatic compounds such as alkaloids and phenolics(Obonga et al., 2019). The FTIR analysis confirms that the *Monodora myristica* seed extract contains a diverse profile of functional groups, including esters, hydroxyl, amine, carbonyl, alkene, aliphatic, and ether groups. These correspond to major phytochemical classes such as fatty acids, terpenoids, flavonoids, triglycerides, phenolic compounds, proteins, alkaloids, and glycosides(Esonu et al. 2020).

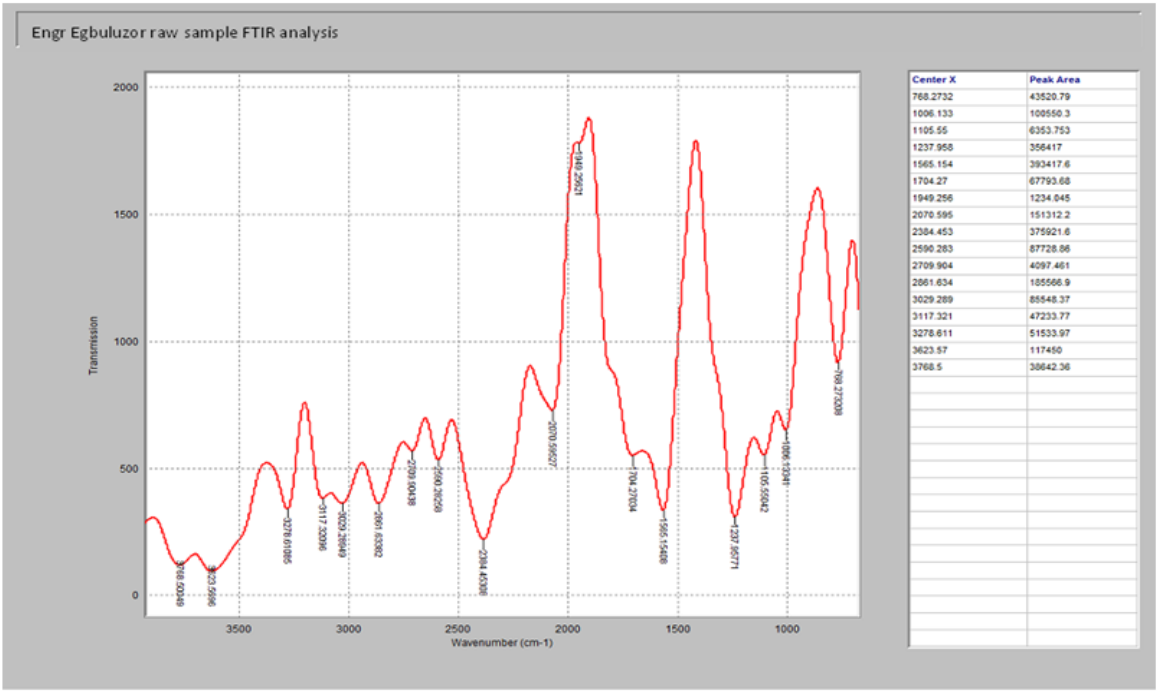

Figure1. FTIR results of the extract of monodora myristica

3.1Paint formulation

The formulated paint was done in two parts. The first part is made up of the resin and other additives, while the second part is the curing agent. The first formulation is the market standard, which is made of epoxy resin as the binder mixed with the other additives in the proportion shown in Table 1 below. The zinc phosphate composition or market standard consists of epoxy resin, Genapol 700, polyethylene glycol (PEG), titanium oxide, zinc phosphate, barite, talc, natrosole, N-butanol, and solvent naphtha. The binder, solvent, and additives were mixed and stirred vigorously until a homogeneous mix was obtained. Also, the extract composition is a mixture of epoxy resin, Genapol 700, polyethylene glycol (PEG), titanium oxide, monodora myristica extract, barite, talc, natrosole, N-butanol, and solvent naphtha. The curing agent comprised N-butanol, solvent naphtha, and versamid 125 mixed vigorously to obtain a homogeneous mix. The two formulations in part A are kept in separate sealed containers, and that of the curing agent part B until ready to use. The two coating formulations (part A) were then mixed separately with the curing agent (part B) in the proportion of 4:1 and were coated on a well-prepared mild steel substrate by spraying, and the sprayed steel coupons were allowed to dry. The coatings as well as the coated substrates, were subjected to mechanical and electrochemical tests. Table 1 shows the weight composition of the standard epoxy coatings containing zinc phosphate and other additives, and epoxy coatings containing the extract and other additives, including the volume percentage of their curing agents. Two coating formulations were prepared. The first coating formulation is an epoxy resin with zinc phosphate coating, and the second formulation is an epoxy resin with monodora myristica extract coating.

Table 1: Coating composition of both zinc phosphate and the extract

S/N	CHEMICALS	ZP COATING	MME COATING
		% WT	COMPOSITION
1.	EPOXY RESIN	24.00	24.00
2	GENAPOL 700	0.50	0.50
3	PEG	0.50	0.50
4	TITANUM OXIDE	15.00	15.00
5	ZINC PHOSPHATE	12.00	-
6	EXTRACT	-	12.00
9	BARRITE	15.00	15.00
10	TALK	10.00	10.00
11	NATROSOL	2.00	2.00
12	N-BUTANOL	7.50	7.50
13	SOLVENT NAPHTHA	13.50	13.50
	TOTAL	100.00	100.00
PART B		% VOL	COMPOSITION
14	VERSAMID 125	40.00	40.00
15	SOLVENT NAPHTHA	40.00	40.00
16	N-BUTANOL	20.00	20.00
	TOTAL	100.00	100.00

3.3 FTIR Analysis of the Coatings

The FTIR spectra of the epoxy coatings containing zinc phosphate in Figure 2 and *Monodora myristica* extract in Figure 3 revealed the characteristic absorption features of the epoxy resin, with distinct variations arising from the incorporated additives. In the zinc phosphate–based coating, a weak broad band around 3400 cm^{-1} corresponded to O–H or N–H stretching vibrations. In contrast, in the *Monodora myristica* extract coating, this band was more intense, indicating the presence of hydroxyl and amine groups from phenolic and other bioactive compounds in the extract. Both spectra displayed aliphatic C–H stretching vibrations in the range of 2850–2950 cm^{-1}, but these were more pronounced in the extract-modified coating, reflecting contributions from fatty acids and terpenoids. The carbonyl and aromatic stretching vibrations observed between 1600–1750 cm^{-1} were sharper in the zinc phosphate system, while in the extract-based coating, the band was broader and more intense, suggesting overlapping contributions from conjugated C=O, C=C, and aromatic structures. In the region of 1000–1300 cm^{-1}, the zinc phosphate coating exhibited well-defined C–O–C stretching associated with the epoxy backbone, alongside characteristic P–O absorptions confirming the presence of the inorganic pigment. Conversely, the extract-modified system showed multiple overlapping peaks in this region, attributable to C–O vibrations of alcohols, esters, and glycosides present in the natural extract. The fingerprint region (500–900 cm^{-1}) further distinguished the two systems with a sharp phosphate-related absorption evident in the zinc phosphate sample, whereas aromatic and alkene bending modes dominated in the *Monodora myristica* coating. The incorporation of zinc phosphate introduced characteristic inorganic phosphate features, whereas the *Monodora myristica* extract enriched the coating with diverse organic functional groups capable of hydrogen bonding and adsorption, thereby suggesting its potential as a sustainable alternative corrosion inhibitor in epoxy-based coatings. Thus, while both systems retain the fundamental epoxy structure, zinc phosphate introduces inorganic protective functionality. In contrast, Monodora *myristica* extract contributes complex organic functional groups that can act synergistically to improve corrosion inhibition.

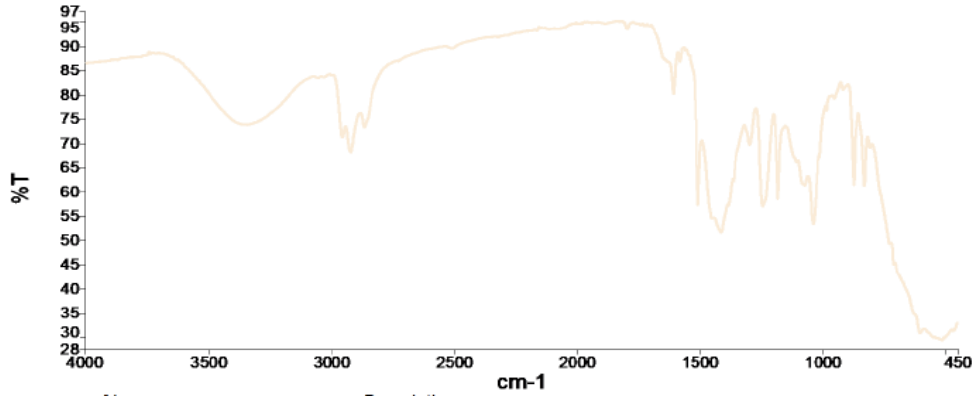

Figure 2 FTIR of the epoxy coating with zinc phosphate

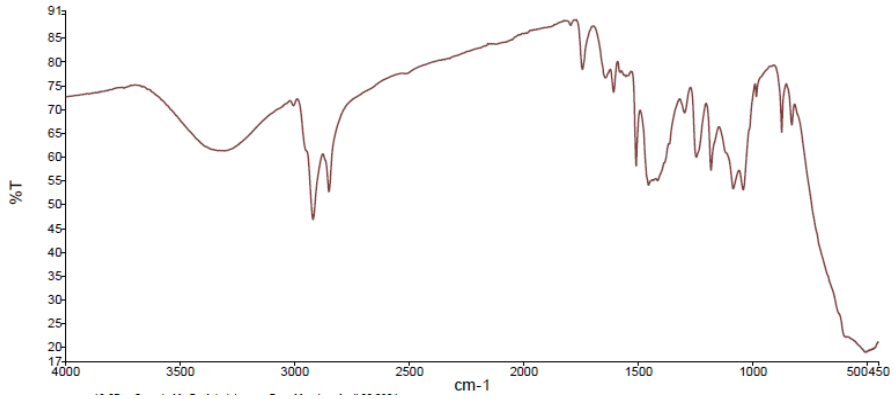

Figure 3 FTIR of the epoxy coating with monodora myristica extract

These spectroscopic distinctions suggest differing mechanisms of corrosion protection. Zinc phosphate coatings protect substrates partly by forming an insoluble, non-conductive phosphate film on steel, essentially acting as a passive barrier(Barsana, Nasar, and Umapathy 2025). Moreover, literature indicates that an optimal zinc phosphate loading (around 30% by volume) yields the best protective capability by facilitating the formation of protective films such as $FePO_4$ and Fe_2O_3(Hao et al., 2013). On the other hand, *Monodora myristica* extract is rich in bioactive organic compounds; its FTIR and phytochemical analyses reveal aromatic, alkyl, ester, and carboxylic functional groups and confirm the presence of phenolics, flavonoids, saponins, and terpenes (Oluwaseyi, Ogede,. These functional groups can serve as adsorption sites that improve barrier properties and inhibit corrosion via physical shielding or chemical interactions. Together, these insights suggest: Zinc phosphate delivers well-defined inorganic protective functionality via passive film formation, while *Monodora myristica* extract contributes multiple organic functional groups that potentially enhance corrosion resistance through hydrogen bonding and adsorption, offering a greener alternative.

3.4 Surface Studies

3.4.1 Atomic Force Microscopy (AFM)

Figures 4 and 5 show the AFM images and Table 2 roughness parameters of the epoxy resin with zinc phosphate coating (ERZC) and that of epoxy resin with extract coating (EREC), respectively. The ERZC exhibited surface roughness of 1.15nm, root mean square (RMS) roughness Sq = 69.56 pm; and sharp asperities (kurtosis = 12.02) when compared with EREC with surface roughness of 0.97nm, root mean square (RMS) roughness 40.86 pm; and sharp asperities (kurtosis = 7.28), The lower values of RMS, confirming that the extract will provide superior protection compared to conventional zinc phosphate. The EREC exhibits lower values of surface roughness, RMS, mean roughness, surface slope, and excess kurtosis, which suggests that its smoother surface will provide a smoother, comparable, and better barrier, along with fewer initiation sites for corrosion. The Inclination (φ) values (355.94° vs. 357.79°) are both very close to 360°/0°, indicating that the overall surface tilt is minimal and nearly perfectly horizontal for both samples.

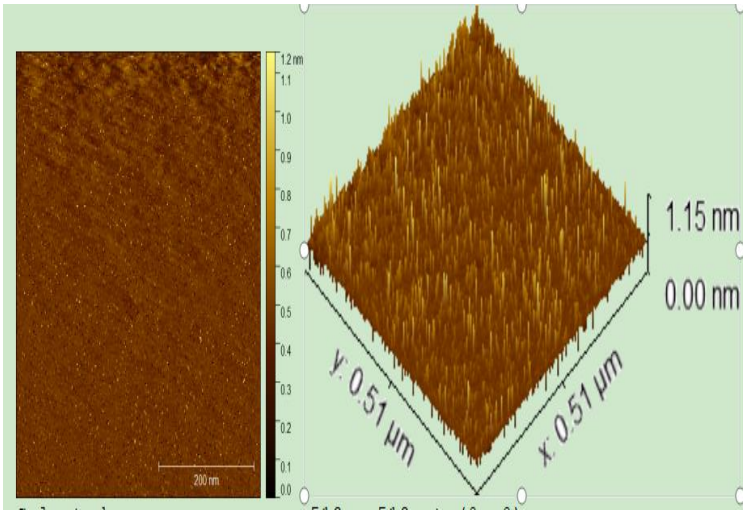

Figure 4 AFM of the epoxy resin with zinc phosphate-coated substrate

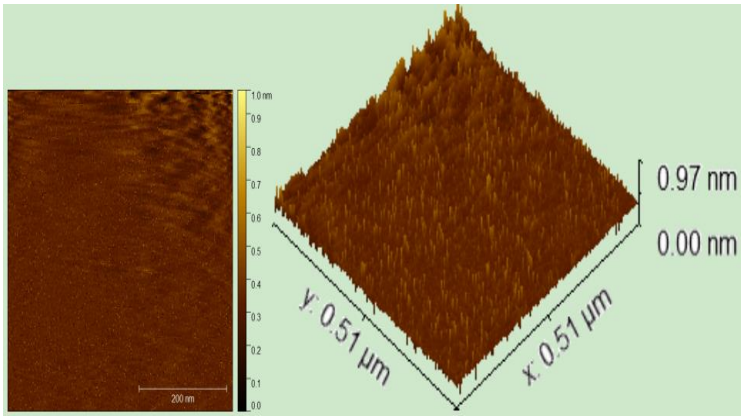

Figure 5 AFM of the epoxy resin with monodora myristica extract-coated substrate

Table 2: AFM roughness parameters

SAMPLE	**ERZC**	**EREC**
Surface Roughness (nm)	1.15	0.97
RMS roughness (Sq)(pm)	69.5599	45.9934
Mean roughness (Sa)(pm)	40.8615	29.5154
Maximum peak height (Sp)(nm)	0.69418	0.630684
Surface slope (Sdq)(nm)	0.0913070	0.0530732
Inclination φ (deg)	355.94	357.79
Skew (Ssk):	0.724497	0.0791887
Excess kurtosis:	12.0201	7.28069
Surface area (nm^2)	263082	262467

3.4.2 Scanning Electron Microscopy (SEM) of the Coated substrate

The surface morphologies of the epoxy resin-zinc phosphate and epoxy resin-extract coated steel substrate are presented in Figures 6 and 7. Figure 6 shows the SEM image of epoxy resin–zinc phosphate coating, while Figure 7 shows the SEM image of epoxy resin-monodora myristica coatings. The microstructure of Figure 6 exhibits visible cracks and discontinuities, which indicate weak surface integrity and the presence of diffusion pathways for aggressive ionic species. Such surface defects may compromise the barrier protection of the coating, thereby accelerating electrolyte penetration and corrosion initiation at the steel/coating interface. However, in Figure 7 surface

appears denser, smoother, and more homogeneous, with fewer cracks or voids compared to the zinc phosphate system. The compact morphology suggests improved film integrity and reduced porosity, which can enhance the barrier effect of the coating. This is because this dense morphology of the extract coating tends to limit ionic diffusion and thus improve long-term corrosion protection of the steel substrate. Although zinc phosphate is a conventional anticorrosive pigment, its dispersion and film formation in this formulation appear to be insufficient in producing a compact, defect-free layer. Nevertheless, the improvement in the surface morphology of Figure 7 can be attributed to the interaction of the extract's organic compounds with the epoxy matrix, which may promote better crosslinking and uniform distribution within the coating(Sheydaei 2024).

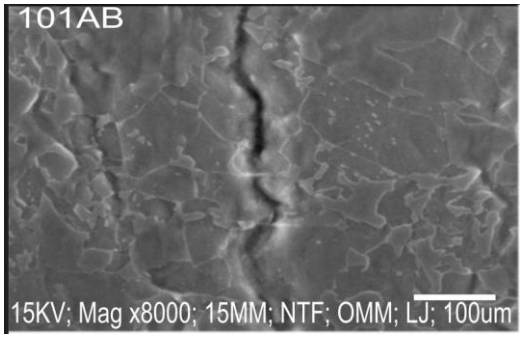

Fig6: SEM images of epoxy resin zinc coatings

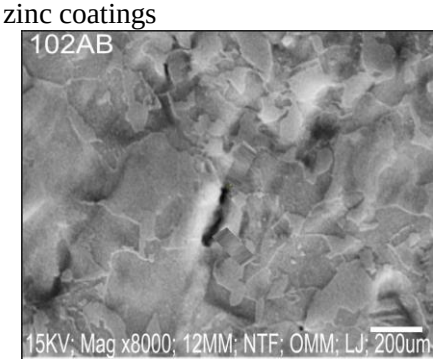

Fig7: SEM images of epoxy resin phosphate coatings

The SEM results indicate that the *Monodora myristica* extract-based epoxy coating provides superior surface compactness and defect minimisation relative to the zinc phosphate formulation. These features are expected to enhance its long-term corrosion protection performance by effectively limiting the ingress of corrosive species to the steel substrate(Ong, Kasi, and Subramaniam 2021).

3.5 Thermal Analysis

The thermogram curves of the epoxy resin-zinc phosphate-coated steel substrate and that of the extract-coated steel substrate are shown in Figures 8 and 9, respectively. Figure 8 shows a significant heat flow magnitude at very high temperatures when compared with Figure 9, which shows the heat flow rising earlier and more steadily, suggesting that it undergoes thermal events at lower temperatures. The DSC thermograms reveal that the zinc phosphate–modified epoxy coating demonstrates superior thermal stability compared to the *Monodora myristica* extract–modified system(Sinko, 2001)[i]. While both coatings exhibit minor low-temperature features (~50–80 °C), the zinc phosphate formulation maintains a gradual heat-flow profile until ~240–260 °C, where rapid decomposition begins. In contrast, the *Monodora* extract coating shows an earlier and steadier increase in heat flow, indicating premature thermal events likely due to the organic nature of the extract. Hence, the zinc phosphate coating is better suited for high-temperature applications, while the *Monodora* extract formulation is more applicable at moderate service temperatures.

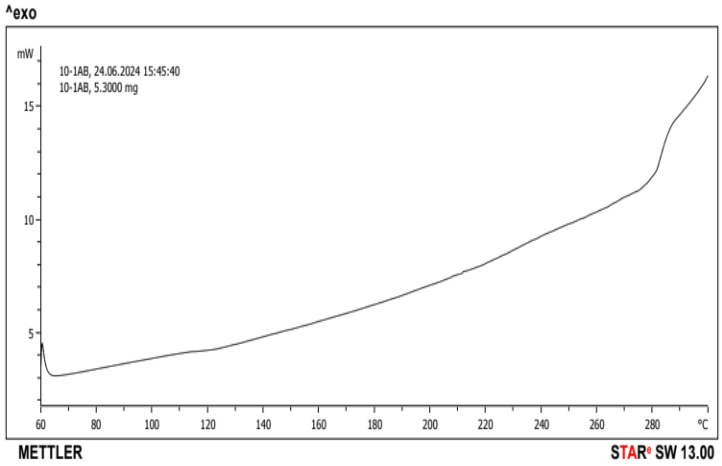

Figure 8: DSC Thermogram plots of epoxy resin phosphate coatings extract coating

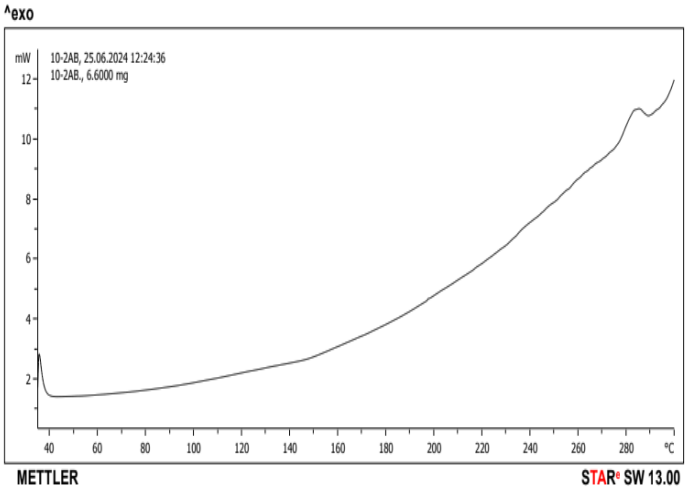

Figure 9: DSC Thermogram plots of epoxy resin monodora myristica extract coating

This study established that both zinc phosphate and *Monodora myristica* extract are effective epoxy coating additives for enhancing corrosion protection on steel substrates, though with different functional strengths. The green extract-based coating demonstrated notable anti-corrosion efficiency, highlighting its potential as a sustainable alternative to conventional inhibitors. However, DSC analysis revealed that the zinc phosphate formulation possesses superior thermal stability, with delayed decomposition onset compared to the *Monodora* extract coating. Consequently, the choice of additive should be application-driven: *Monodora myristica* extract is most suitable for eco-friendly corrosion protection in moderate service conditions. At the same time, zinc phosphate remains more reliable for high-temperature or thermally demanding environments.

3.6 Mechanical Properties

The Rockwell B hardness values of the epoxy resin–coated steel substrates are presented in Table 3. Both coating systems were tested under identical conditions using a 1/16″ diameter hardened steel ball indenter and a 100 kgf load. As shown in Table 3.

Table 3: Micro hardness tests of the epoxy resin-coated steel substrates

S/N	NUMENCLATURE OF SAMPLES	SCALE (X)	ABBREVIATION	LOAD	INDENTER	ROCKWELL HARDNESS VALUES
1	epoxy resin-zinc phosphate-coated steel substrate	B	HRB	100kgf	1/16 diameter. Hardened Steel Ball	99.2 HR
2	epoxy resin-extract-coated steel substrate	B	HRB	100kgf	1/16 diameter. Hardened Steel Ball	100.3HR

The hardness results for both epoxy resin-coated steel substrates (99.2-100.3 HRB) show that the coatings created mechanically stable surfaces without reducing the inherent hardness of the steel. Hardness can indicate coating integrity since harder or better-adhered coatings resist indentation, abrasion, and micro-damage. These factors often start corrosion. The zinc phosphate-treated sample, with a hardness of 99.2 HRB, was slightly softer than the extract-based sample. This small difference might suggest a coating system that absorbs and distributes stress better. The extract-based pretreatment had a slightly higher hardness value (100.3 HRB), indicating a stiffer surface layer. The close hardness values confirm that both coating systems produce strong surfaces that offer protective coverage.

3.7 Rapid electrochemical assessment of paints (REAP)

The rapid electrochemical assessment of paint (REAP) parameters for epoxy resin coatings developed with zinc phosphate and plant extract (Monodora myristica) are shown in Table 4. Among the parameters taken into account are the following: disbonding rate (dx/dt), coating capacitance at zero immersion (Cc0) and after 24 hours of soaking (Cc24), corrosion resistance (Rcorr), coating water uptake (%V), and the estimated relative time to failure (TTF).

Table 4 REAP parameters for epoxy resin coated with zinc phosphate and extracts

Coated Steel Surface with	Corrosion resistance Rcorr (ohms)	Coating capacitance at zero hour, C_{c0} (F)	Coating capacitance after 24 hours soak time, C_{c24} (F)	Coating water update, %V	Disbonding rate, dx/dt(mm/h)	Relative Time To Failure, TTF(hrs)
Epoxy resin coatings with zinc phosphate	7.4275	0.0055	0.0348	-42.10060	2.08	1240.94
Epoxy resin coatings with extract	5.9851	1.51E-05	8.30E-05	-38.92885363	1.75	1090.23

The predictive service life based on REAP calculations (TTF) was longer for the zinc phosphate formulation (1240.9 h) than for the extract-modified coating (1090.2 h). This is due to the superior inhibition of electrochemical processes at the coating/metal interface, resulting from the high Rcorr of the zinc phosphate-modified coating compared to extract-based coatings. This is because higher corrosion resistance corresponds to lower ionic conductivity and more potent barrier properties. This outcome reflects the conventional role of inorganic pigments (zinc phosphates, etc.) in extending coating durability [Tran et al., 2025]. Nevertheless, the extract-based coating demonstrated competitive long-term performance, particularly in its resistance to water ingress and slower disbonding rate, which are critical for sustained barrier protection. Overall, these findings suggest that while zinc phosphate remains a more effective inhibitor in terms of absolute corrosion resistance and service life, Monodora *myristica* extract provides significant barrier reinforcement and adhesion benefits. The extract's performance underscores its potential as a sustainable, eco-friendly alternative to conventional chromate-free anticorrosive pigments, consistent with emerging trends in green corrosion protection strategies.

The zinc phosphate formulation had a longer predictive service life (1240.9 h) based on REAP calculations (TTF) than the extract-modified coating (1090.2 h). This is because the zinc phosphate-modified coating's high Rcorr, when compared to extract-based coatings, results in superior inhibition of electrochemical processes at the coating/metal interface. This is because stronger barrier qualities and reduced ionic conductivity are correlated with increased corrosion resistance. This result illustrates how inorganic pigments, such as zinc phosphates, are traditionally used to increase coating durability [Tran et al., 2025]. However, the extract-based coating showed competitive long-term performance, especially in its slower disbonding rate and resistance to water ingress, both of which are essential for long-lasting barrier protection. These results indicate that Monodora myristica extract offers considerable barrier reinforcement and adhesion benefits. However, zinc phosphate is still a more effective inhibitor in terms of absolute corrosion resistance and service life. The extract's performance highlights its potential as an environmentally friendly and sustainable substitute for traditional chromate-free anticorrosive pigments, aligning with new developments in green corrosion prevention techniques.

3.8 Computational Studies

3.8.1 Density Functional Theory (DFT)

Density functional theory calculations were performed to investigate the adsorption of a cured epoxy resin with versamid, zinc phosphate and three molecular representatives of Monodora-Myristica extract on the Fe(110) surface. The frontline molecular orbitals were used to determine the coatings' anticorrosion characteristics. The energy of the highest occupied molecular orbitals (E_{HOMO}), which is the ability of the organic compound to donate electrons to the shielded metal, and that of the lowest unoccupied molecular orbital (E_{LUMO}), being the ability of the compound to accept electrons from the metal's conducting band, are used to assess the reactivity of the coating compounds. The optimised structures of the coating molecules showing electron density distribution of the HOMO and LUMO are displayed in Figure 10. The values of E_{HOMO} and E_{LUMO} are shown in Table 5. From these values, other molecular descriptors like electronegativity, ionisation potential, electron affinity, etc., were calculated using DFT to evaluate the anti-corrosion behaviour of the inhibitor molecules as shown in equations 4-12(Aiman et al., 2025).

$$\Delta E = \text{Energy gap} = (E_{LUMO} - E_{HOMO}) \quad (4)$$

$$IP = \text{ionization potential} = -E_{HOMO}\ (eV) \quad (5)$$

$$EA = \text{Electron affinity} = -E_{LUMO}\ (eV) \quad (6)$$

$$\chi = \text{Electronegativity} = \left(\frac{IP+EA}{2}\right)\ (eV) \quad (7)$$

$$\mu = \text{global chemical potential} = -\chi = -\left(\frac{IP+EA}{2}\right)\ (eV) \quad (8)$$

$$\eta_N = \text{Global hardness}\ \frac{(1P-EA)}{2} \quad \mu^- = -\frac{(3I-A)}{4} \quad \mu^+ = -\frac{(I-3A)}{4}\ (eV) \quad (9)$$

$$\sigma = \text{Global softness} = \frac{1}{\eta_N}\ (eV) \quad (10)$$

$$\omega = \text{Electrophilicity index} \approx \frac{(I+A)^2}{8(I-A)} = \frac{\mu^2}{2\eta_N} = \frac{\chi^2}{2\eta_N}\ (eV) \quad (11)$$

$$\varepsilon = \text{nucleophilicity} = \frac{1}{\omega}\ (eV) \quad (12)$$

Table 5. Values of the energies of the highest occupied molecular orbitals (E_{HOMO}), and that of the lowest unoccupied molecular orbital (E_{LUMO}) and other discriptors in electron volts (eV)

Materials	Epoxy-versamid	Zinc phosphate	Hepta-fluorobutanoate	9-octadecenoc acid methyl esther	Methyl stearate
E_{HOMO}	-5.171	-6.536	-5.607	-4.698	-6.434
E_{LUMO}	−1.235	−5.340	−2.521	−2.964	−1.078
Energy gap (**ΔE**)	3.936	1.196	3.086	1.734	5.356
Ionization potential (IP)	5.171	6.536	5.607	4.698	6.434
Electron affinity (EA)	1.235	5.340	2.521	2.964	1.078
Electronegativity (χ)	3.203	5.938	4.064	3.831	3.756
Global chemical potential (**μ**)	−3.203	−5.938	−4.064	−3.831	−3.756
Global hardness (**η**)	1.968	0.598	1.543	0.867	2.678
Global softness S (1/**η**)	0.5081	1.6722	0.6481	1.1534	0.3734
Electrophilicity index	2.6065	29.4815	5.3519	8.4640	2.6340
nucleophilicity	0.3837	0.0339	0.1868	0.1181	0.3797

The computed global reactivity descriptors in Table 5 shed more light on the compounds' mechanism of inhibition. According to the energy gap (ΔE) values, methyl stearate (5.356 eV) had the lowest chemical reactivity, while zinc phosphate (1.196 eV) and 9-octadecenoic acid methyl ester (1.734 eV) had the highest. Zinc phosphate and methyl stearate showed the highest values (>6 eV), indicating weaker donation, while the ester had the lowest ionisation potential (IP) (4.698 eV), indicating strong electron-donating ability. In contrast, the organic inhibitors displayed moderate values of electron affinity (EA), whereas zinc phosphate had the highest EA (5.340 eV), which is consistent with its strong electron-accepting nature. With zinc phosphate (5.938 eV) being the most electron-withdrawing and epoxy-versamid and the esters remaining within a moderate range (~3–4 eV), the calculated electronegativity (χ) showed a similar pattern. Zinc phosphate (η = 0.598 eV, S = 1.67 eV^{-1}) and the ester (η = 0.867 eV, S = 1.15 eV^{-1}) were found to be the softest, making them the most capable of polarisation and charge transfer at the steel surface. The hardest substance, on the other hand, was methyl stearate (η = 2.678 eV). Because of its strong propensity to accept electrons, zinc phosphate had a significantly higher electrophilicity index (ω) (29.5 eV). Conversely, methyl stearate

and epoxy-versamid displayed comparatively low values (~2.6 eV), indicating donor-dominated behaviour. According to the descriptors, zinc phosphate primarily serves as a strong electron acceptor, allowing back-donation from the metal. At the same time, epoxy-versamid and the organic esters primarily act as electron donors, improving chemisorption through donation to vacant d-orbitals of steel.

S/N	COMPOUND	OPTIMIZED STRUCTURE	HOMO OBITAL	LOMO ORBITAL
1	EPOXY - VERSAMID	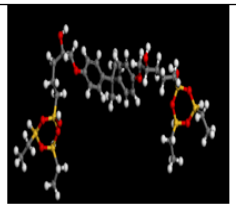	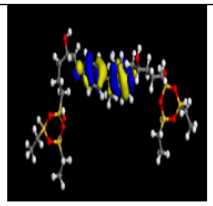	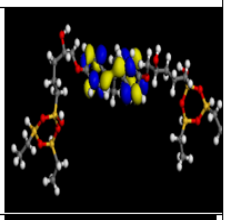
5	Zinc Phosphate	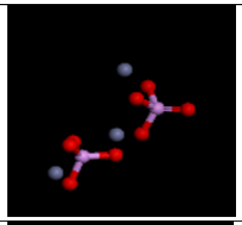	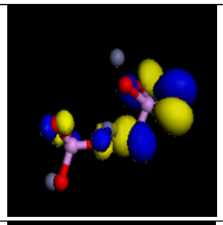	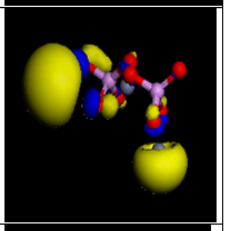
6	Heptafluorobutanoate	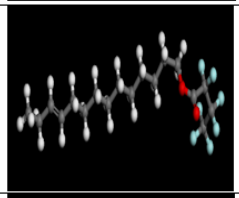	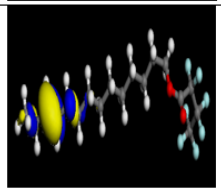	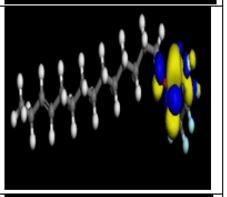
8	9-octadecenoic acid methyl ester	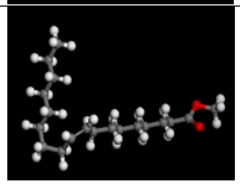	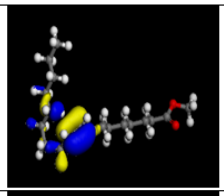	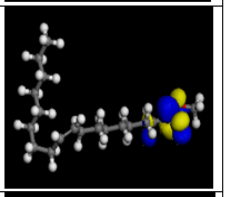
9	Methyl stearate	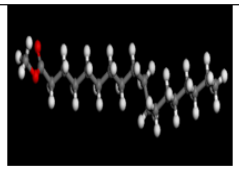	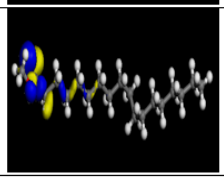	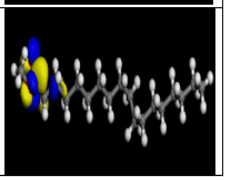

Figure 10: Optimised structures of the coating molecules showing electron density distribution of the HOMO and LUMO

3.8.2 Molecular Dynamics Simulations (MDS):

Figure 11 shows the adsorption energies of the two coating formulations on mild steel, which were found using Forcite quench simulations. When zinc phosphate was added to epoxy resin coatings, the adsorption energy was –23.229 kcal/mol. When the extract was added, the value was slightly more negative at –24.898 kcal/mol. Adsorption energy is a crucial factor in determining the strength of the interaction between inhibitor molecules and metal surfaces. More negative values mean stronger and more stable adsorption. The relatively high negative adsorption energy of Epoxy resin coatings with zinc phosphate indicates that the coating molecules adhere firmly to the steel surface, thereby creating a protective layer that hinders the access of corrosive ions to the steel. However, the adsorption energy of Epoxy resin coatings with extract is lower, indicating that they interact more strongly with the steel surface. This better adsorption makes the inhibitor layer more stable, covers more surface area, and blocks active corrosion sites more effectively.
These results indicate that both coatings adhere to the steel surface; however, epoxy resin coatings with extract offer superior corrosion protection due to their enhanced adhesion. The better adsorption behavior is linked to the creation of a compact and stable barrier film, which works better as a shield against aggressive species in the corrosive environment.

NAME	STRUCTURE(SIDE VIEW)	TOP VIEW	ADSORPTION ENERGY
Epoxy resin coatings with zinc phosphate	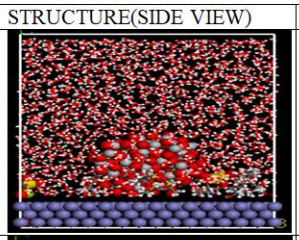	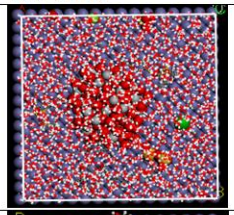	-23.229 Kcal/mol
Epoxy resin coatings withmonodora myrista extract	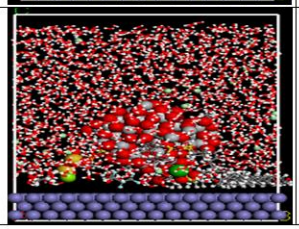	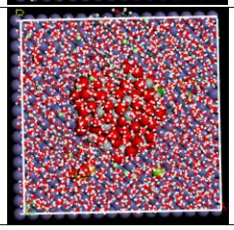	-24.898 Kcal/mol

Fig 11: Adsorption of coating different formulations on mild steel surface after Forcite quench simulation with its adsorption energies.

The DFT descriptors and adsorption studies show that effective corrosion inhibition happens when strong electron donor species (epoxy versamid and fatty acid esters) and electron acceptors (zinc phosphate) work together. This enhances surface charge transfer and maintains the stability of the adsorbed layer. The higher adsorption energy of epoxy resin coatings with the extract indicates its enhanced protective capabilities, aligning with its favourable electronic reactivity profile and suggesting it could be a superior anti-corrosion coating formulation.

4.0 CONCLUSIONS

Monodora myristica extract is a viable, sustainable substitute for zinc phosphate in epoxy coatings, offering environmentally friendly corrosion protection without significantly compromising performance.

Both zinc phosphate and MME-enhanced coatings demonstrated effective anticorrosion properties, with zinc phosphate providing longer service life and stronger barrier qualities. At the same time, MME contributed to barrier reinforcement, adhesion, and eco-friendliness.
Morphological and thermal studies indicated comparable surface roughness and thermal stability between zinc phosphate and MME coatings, suggesting that MME does not compromise these properties.

Electrochemical assessments showed that MME-coated epoxy has resistance closely comparable to zinc phosphate, reinforcing its potential as an effective corrosion inhibitor.

The study supports the feasibility of using Monodora myristica extract as a green, biodegradable alternative to traditional inorganic corrosion inhibitors in epoxy-based coatings, with performance characteristics suitable for practical applications. Incorporating MME aligns with sustainable development goals, as it reduces reliance on toxic inorganic inhibitors and utilises renewable plant resources, thus lowering environmental impact.

Acknowledgments
The authors duly acknowledged the support from the second Higher Education Centres of Excellence for Development Impact (ACE-Impact) Project—P16906-4A No 6510-NG, funded by the World Bank and Federal University of Technology, Owerri, Imo State, Nigeria.

Declaration of competing interests
The authors have no competing interests to declare that are relevant to the content of this article.

Funding
This research received no external funding.

Author contributions:
All authors contributed to the study's conception and design. Egbuhuzor Macdenis Onyekachi and Chris Akalezi performed material preparation, data collection and analysis. Egbuhuzor Macdenis Onyekachi and Chris Akalezi did all the laboratory work and wrote the first draft of the manuscript, and all authors reviewed and commented on previous versions. Chris Akalezi, Chinyere Ada Madu, and Emeka Oguzie supervised the work. All authors read and approved the final manuscript.

Ethics, consent to participate and consent to publish
Ethics, Consent to Participate, and Consent to Publish declarations: not applicable.

REFERENCES

Aiman, Nur, Najwa Kamarul, Sheikh Ahmad, Izaddin Sheikh, Fazira Ilyana, Abdul Razak, Siti Syaida Sirat, Amalina Mohd, Siti Radiah, Mohd Kamarudin, and Nur Nadia Dzulkifli. 2025. "Hirshfeld , Surface Analysis , DFT and Corrosion Inhibition Mechanism of Vanillin 4-Ethylthiosemicarbazone on Mild Steel in 1M HCl." *Moroccan Journal of Chemistry* 13(1):80–105.

Al-Amiery, Ahmed A., Wan Nor Roslam Wan Isahak, and Waleed Khalid Al-Azzawi. 2023. "Corrosion Inhibitors: Natural and Synthetic Organic Inhibitors." *Lubricants* 11(4):174. doi: 10.3390/lubricants11040174.

Bansal, Poonam, Sunayna Choudhary, Tanvi Taneja, Sonali Sangwan, Bhupesh Gupta, Soniya Goyal, Raman Kumar, and Pooja Sharma. 2016. "We Are IntechOpen , the World ' s Leading Publisher of Open Access Books Built by Scientists , for Scientists TOP 1 %." *Intech* i(tourism):15. doi: http://dx.doi.org/10.5772/intechopen.72943.

Barsana, S. Ayesha, A. Sultan Nasar, and M. J. Umapathy. 2025. "Enhanced Corrosion Resistance of Zinc Phosphate Coatings on Mild Steel through Incorporation of Nanocrystalline CeO 2 and CeO 2 –CuO Nanocomposite." *RSC Advances* 15(26):20916–34. doi: 10.1039/D5RA02800K.

Bastidas, David M. 2020. "Corrosion and Protection of Metals." *Metals* 10(4):458. doi: 10.3390/met10040458.

Buchheit, R. G., M. Cunningham, H. Jensen, M. W. Kendig, and M. A. Martinez. 1998. "A Correlation Between Salt Spray and Electrochemical Impedance Spectroscopy Test Results for Conversion-Coated Aluminum Alloys." *Corrosion* 54(1):61–72. doi: 10.5006/1.3284829.

Egbuhuzor, O. M., I. C. Madufor, S. C. Nwanonenyi, and J. O. Bokolo. 2020. "Adsorption Behavior and Corrosion Rate Model of Sodium Carboxymethyl Cellulose (Na-CMC) Polymer on Aluminium in HCl Solution." *Nigerian Journal of Technology* 39(2):369–78. doi: 10.4314/njt.v39i2.7.

Esonu, B. O., U. D. Ogbonna, G. A. Anyanwu, U. H. Ukpabi, F. C. Azubuike, and V. Odoemelam. 2020. "Chemical and Nutritive Evaluation of Jatropha Curcas Leaf Meal in Broiler Chicken Diets." *Nigerian Journal of Animal Production* 47(4):176–83.

Hansson, C. M. 2011. "The Impact of Corrosion on Society." *Metallurgical and Materials Transactions A: Physical Metallurgy and Materials Science* 42(10):2952–62. doi: 10.1007/s11661-011-0703-2.

Hao, Yongsheng, Fuchun Liu, En-Hou Han, Saima Anjum, and Guobao Xu. 2013. "The Mechanism of Inhibition by Zinc Phosphate in an Epoxy Coating." *Corrosion Science* 69:77–86. doi: 10.1016/j.corsci.2012.11.025.

Humar, M. 2017. "Protection of the Bio-Based Material." Pp. 187–247 in *Performance of Bio-based Building Materials*. Elsevier.

Leite, Adriana O. S., Walney S. Araújo, Isabel C. P. Margarit, Adriana N. Correia, and Pedro de Lima-Neto. 2005. "Evaluation of the Anticorrosive Properties of Environmental Friendly Inorganic Corrosion Inhibitors Pigments." *Journal of the Brazilian Chemical Society* 16(4):756–62. doi: 10.1590/S0103-50532005000500013.

Nguyen, Khang Duy Huu, Tran Dinh Manh, Bui Xuan Vuong, Lien Thi Phuong Nguyen, Dao Thanh Vu, Thanh Liem Huynh, and Kim Long Duong Ngo. 2024. "Syzygium Polyanthum (Wight) Walp. Leaf Extract as a Sustainable Corrosion Inhibitor for Carbon Steel in Hydrochloric Acidic Environment." *Journal of Industrial and Engineering Chemistry*. doi: 10.1016/j.jiec.2024.08.054.

Obonga, Wilfred O., Edwin O. Omeje, Charles O. Nnadi, and Wilson G. Ocheme. 2019. "Phytochemical Evaluation of Extracts and GC-MS Analysis of Oil from Monodora Myristica

Seed." *Dhaka University Journal of Pharmaceutical Sciences* 18(1):69–73. doi: 10.3329/dujps.v18i1.41893.

Ong, Gerard, Ramesh Kasi, and Ramesh Subramaniam. 2021. "A Review on Plant Extracts as Natural Additives in Coating Applications." *Progress in Organic Coatings* 151(August 2020):106091. doi: 10.1016/j.porgcoat.2020.106091.

R. Holla, Bhoomika, R. Mahesh, H. R. Manjunath, and V. Raghu Anjanapura. 2024. "Plant Extracts as Green Corrosion Inhibitors for Different Kinds of Steel: A Review." *Heliyon* 10(14):e33748. doi: 10.1016/j.heliyon.2024.e33748.

Sahu, Meena, and Kk Haris. 2017. "Phytochemical Analysis of the Leaf , Stem and Seed Extracts of Cajanus Cajan L (Dicotyledoneae : Fabaceae) PHYTOCHEMICALANALYSIS OF THE LEAF , STEM AND SEED EXTRACTS OF CAJANUS CAJAN L (DICOTYLEDONEAE : FABACEAE)." *WORLD JOURNAL OF PHARMACY AND PHARMACEUTICAL SCIENCES* (March).

Sheydaei, Milad. 2024. "The Use of Plant Extracts as Green Corrosion Inhibitors: A Review." *Surfaces* 7(2):380–403. doi: 10.3390/surfaces7020024.

Singh, Ambrish, Eno E. Ebenso, and M. A. Quraishi. 2012. "Corrosion Inhibition of Carbon Steel in HCl Solution by Some Plant Extracts." *International Journal of Corrosion* 2012. doi: 10.1155/2012/897430.

Sinko, John. 2001. "Challenges of Chromate Inhibitor Pigments Replacement in Organic Coatings." *Progress in Organic Coatings* 42(3–4):267–82. doi: 10.1016/S0300-9440(01)00202-8.

Sørensen, P. A., S. Kiil, K. Dam-Johansen, and C. E. Weinell. 2009. "Anticorrosive Coatings: A Review." *Journal of Coatings Technology and Research* 6(2):135–76. doi: 10.1007/s11998-008-9144-2.